Journal of Applied and Computational Mechanics, Vol. 1, No. 3, (2015), 112-121
DOI: 10.22055/jacm.2015.10935

Journal of
Applied and Computational Mechanics

Effect of thermoelastic damping in nonlinear beam model of MEMS resonators by differential quadrature method

Nassim Ale Ali[1], Ardeshir Karami Mohamadi[2]

[1]Department of Marine Engineering, Khorramshahr University of Marine Science & Technology
Khorramshahr, 43175-64199, Iran, aleali@kmsu.ac.ir,
[2]Department of Mechanical Engineering, Shahrood University of Technology, Shahrood
Shahrood, Iran, akarami@yahoo.com

Received October 12 2014; revised December 08 2014; accepted for publication January 08 2015.
Corresponding author: Nassim Ale Ali, aleali@kmsu.ac.ir

Abstract

This paper presents a nonlinear model of a clamped-clamped microbeam actuated by an electrostatic load with stretching and thermoelastic effects. The frequency of free vibration is calculated by discretization based on the Differential Quadrature (DQ) Method. The frequency is a complex value due to the thermoelastic effect that dissipates energy. By separating the real and imaginary parts of frequency, the quality factor of thermoelastic damping is calculated. Both the stretching and thermoelastic effects are validated by the referenced papers. This paper shows that the main nonlinearity of this model is voltage, which makes the difference between linear and nonlinear models. The variation of thermoelastic damping (TED) versus geometrical parameters, such as thickness, gap distance and length, is investigated and these results are compared by linear and nonlinear models in high voltages. This paper also shows that in high voltages the linear model has a large margin of error for calculating thermoelastic damping (TED) and thus the nonlinear model should be used.

Keywords: thermoelastic damping, stretching effect, resonator, differential quadrature method.

1. Introduction

In MEMS, there are kinds of damping which affect the performance of the devices. These damping are divided by two parts: a) extrinsic b) intrinsic. Extrinsic damping can be weakened by suitable design, proper methods of fabrication and appropriate operating conditions. For example, squeeze film damping is the extrinsic damping that can be minimized by encapsulating the devices [1, 2].

Thermoelastic damping (TED) that increases with miniaturization of devices is the intrinsic damping in MEMS [1]. The intrinsic damping cannot be weakened by suitable design, proper methods of fabrication and appropriate operating conditions [2]. The first who predicted the thermoelastic damping was Zener [3, 4]. Alblas [5] treated conversion of mechanical energy into heat in vibrating elastic beam. He found that this damping for macro structures is negligible. Lifshitz and Roukes [6] obtained the quality factor of thermo-elastic beam in micro scale and found that thermoelastic damping in micro and nano scales is important.

For calculating the quality factor of thermoelastic damping, there are two methods: energy method and eigenfrequency method. In the energy method, dissipated and maximum stored energy should be calculated (for example see [7, 8, 9, and 10]) and in the eigenfrequency method, real and imaginary parts of eigenfrequency should be calculated (for example see [1, 11, 12, and 13]). Each method can be done with numeric or analytic procedures or combination of them.

Nayfeh and Mohammed [1] modeled an electrostatically microplate by considering TED. They obtained an expression for quality factor analytically by using a perturbation approach. Sun and Saka [11] derived an analytical

expression of thermoelastic damping for circular microplate. They also obtained a critical thickness that represents the maximum damping.

In MEMS, there are different actuating and sensing mechanisms such as thermal, optical, electrostatic, electromagnetic, piezoresistive and piezoelectric but electrostatic actuation is often preferred [14]. In electrostatic actuation an elastic conductor is located above a stationary conductor. The electrical load is composed of two components, including AC and DC voltage. The applied DC voltage deforms the upper elastic surface that causes to change in the system capacitance and to stretch the mid-plane of the elastic surface.

There are many phenomena which appear in nano scales such as van der Waals interaction, Casimir force, size dependency of the mechanical performance of nano structures [40], surface residual stress and surface stiffness [39] but in this paper, these forces and phenomena are ignored due to investigating TED in the micro-beam.

There are a number of studies investigating the electrical actuation in micro structures. Batra and et al. reviewed them in [15]. In their review, many works of Nayfeh and et al. are seen [16-24]. In one of them, Nayfeh and et al. [16] presented a nonlinear model of electrically actuated microbeams considering mid-plane stretching.

Accordingly MEMS resonators are devices that vibrate with AC voltage around the static deflection that is due to DC polarization voltage. The thermoelastic damping as well as frequency of structure of resonator is affected by the DC voltage because the thermoelastic damping is directly related to imaginary part of frequency [7]. In addition, in MEMS resonators, high sensitivity and resolution are needed [2] so to achieve this purpose, the damping in such devices should be decreased. However, studying the behavior of thermoelastic damping in resonators is necessary for manufactures of MEMS.

The differential quadrature (DQ) method was first introduced by Belman and Casti [25]. This numerical technique is employed in many nonlinear problems such as nonlinear free vibration of isotropic beams and orthotropic plates [26-32]. Also, Malekzadeh used DQ method for solving large amplitude free vibration of laminated skew plate, [33] tapered plate, [34] thick functionally graded plate [35] and composite beams [36].

In this paper, a nonlinear model of clamped-clamped microbeam actuated by electrostatic load with stretching and thermoelastic effects is presented. The frequency of free vibration is calculated by discretization based on DQ method. In this method, the differentiations are approximated by linear algebraic expressions. The frequencies are a complex values due to the thermoelastic effect that dissipates the energy. The frequencies are obtained by iteration for a silicon microbeam and by separating the real and imaginary parts of frequencies. The quality factor of thermoelastic damping is calculated in the first mode of free vibration. Both stretching and thermoelastic effects are validated by papers in reference. This paper shows that the main nonlinearity of this model is the voltage that makes the difference between linear and nonlinear model. The variation of TED versus geometrical parameters such as thickness, gap distance and length is investigated and these results are compared using linear and nonlinear models at high values of voltage. Furthermore, this paper shows that at high values of voltages, the linear model has large error for calculating the TED and for this reason the nonlinear model should be used.

2. Modeling

The resonator, the figure 1, is modeled as a microbeam bending under the electrostatic load which is a DC voltage (polarization voltage) V_p. This electrostatic load is uniform along the width of microbeam and is applied by a uniform parallel electrode lying under the microbeam without fringing field effect. The microbeam is also clamped at both ends. $w(x,t)$ is defined as the transverse deflection of the beam. The vibration equation of nonlinear thermo-elastic beam considering mid-plane stretching is derived by adding thermal moment, M^T, and thermal axial force, N^T, in "Nonlinear 2-D Euler-Bernoulli Beam Theory" with stretching effect which is presented in [37].

$$\rho A\frac{\partial^2 w}{\partial t^2}+EI\frac{\partial^4 w}{\partial x^4}+\frac{\partial^2 M^T}{\partial x^2}=\frac{\partial^2 w}{\partial x^2}\left\{P(t)-\frac{1}{L}\int_0^L\left[\left(N^T-\frac{\partial M^T}{\partial x}\frac{\partial w}{\partial x}\right)-\frac{EA}{2}\left(\frac{\partial w}{\partial x}\right)^2\right]dx\right\}+\frac{1}{2}\epsilon b\frac{{V_p}^2}{(d-w)^2} \quad (1)$$

Where

$$M^T=E\alpha_T b\int z\theta dz \quad (2)$$

$$N^T=E\alpha_T b\int \theta dz \quad (3)$$

where $\theta=T-T_0$ in which $T(x,z,t)$ and T_0 are defined as temperature field of the beam and stress-free temperature (in equilibrium) respectively. Also, t, α_T, E, $P(t)$, L, b, d, ϵ and ρ are time, coefficient of thermal expansion, Young's modulus, applied axial force, length, width, the gap distance, the dielectric constant and the material density, respectively. It is noted that the cross section of the microbeam is rectangular, thus the area and moment of inertia of the cross section are $A=bh$ and $I=bh^3/12$ where h is the thickness.

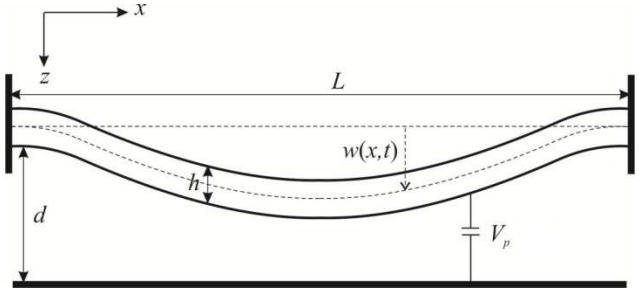

Fig. 1. Schematic of electrically actuated resonator.

In the thermal model, Lifshitz and Roukes [6] assumption is used so the thermal gradient in the z direction is much larger than gradient in x direction. The thermal conduction equation, containing the thermoelastic coupling term, can be written as following.

$$\kappa\frac{\partial^2\theta}{\partial z^2}=\rho c_v\frac{\partial\theta}{\partial t}-\beta T_0 z\frac{\partial}{\partial t}\left(\frac{\partial^2 w}{\partial x^2}\right) \tag{4}$$

Where c_v and κ are specific heat at constant volume and the thermal conductivity, respectively and $\beta=E\alpha_T/(1-2\nu)$ is thermal modulus where ν is the Poisson ratio.

So the equations (1) and (4) represent the governing equations of nonlinear vibration of microbeam with TED. In addition, thermal and elastic properties are independent from temperature and the temperature change due to TED is assumed small thus the vibration of microbeam is investigated around a constant temperature, in this case this temperature is considered T_0.

For convenience, the nondimensional variables are introduced (denoted by hats)

$$\hat{w}=\frac{w}{d},\quad \hat{x}=\frac{x}{L},\quad \hat{t}=\frac{t}{\bar{t}},\quad \hat{z}=\frac{z}{h},\quad \hat{\theta}=\frac{\theta}{\bar{\theta}} \tag{5}$$

Where $\bar{t}=\sqrt{\frac{\rho bhL^4}{EI}}$ and $\bar{\theta}=\frac{\beta T_0 dh^3}{\kappa\bar{t}L^2}$. Substituting equation (5) into equation (1) and (4), the following equation is obtained

$$\frac{\partial^2\hat{w}}{\partial\hat{t}^2}+\frac{\partial^4\hat{w}}{\partial\hat{x}^4}+\alpha_1\frac{\partial^2\hat{M}^T}{\partial\hat{x}^2}=\frac{\partial^2\hat{w}}{\partial\hat{x}^2}\left\{\hat{P}(t)-\int_0^1\left[\alpha_6\hat{N}^T-\alpha_2\frac{\partial\hat{M}^T}{\partial\hat{x}}\frac{\partial\hat{w}}{\partial\hat{x}}-\alpha_3\left(\frac{\partial\hat{w}}{\partial\hat{x}}\right)^2\right]d\hat{x}\right\}+\alpha_4\frac{{V_p}^2}{(1-\hat{w})^2} \tag{6}$$

$$\frac{\partial^2\hat{\theta}}{\partial\hat{z}^2}=\alpha_5\frac{\partial\hat{\theta}}{\partial\hat{t}}-\hat{z}\frac{\partial}{\partial\hat{t}}\left(\frac{\partial^2\hat{w}}{\partial\hat{x}^2}\right) \tag{7}$$

Where

$$\alpha_1=\frac{12\alpha_T\bar{\theta}L^2}{hd},\quad \alpha_2=\frac{12\alpha_T\bar{\theta}d}{h},\quad \alpha_3=\frac{6d^2}{h^2},\quad \alpha_4=\frac{6\epsilon L^4}{Eh^3d^3},\quad \alpha_5=\frac{\rho c_v h^2}{\bar{t}\kappa},\qquad \alpha_6=\frac{12L^2\alpha_T\bar{\theta}}{h^2} \tag{8}$$

$$\hat{M}^T=\int_{-\frac{1}{2}}^{\frac{1}{2}}\hat{z}\hat{\theta}d\hat{z},\quad \hat{N}^T=\int_{-\frac{1}{2}}^{\frac{1}{2}}\hat{\theta}d\hat{z},\quad \hat{P}(t)=\frac{L^2}{EI}P(t) \tag{9}$$

Boundary conditions at the boundaries of beam are as following

$$w(0,t)=w(L,t)=0,\quad \left.\frac{\partial w}{\partial x}\right|_{(0,t)}=\left.\frac{\partial w}{\partial x}\right|_{(L,t)}=0 \tag{10}$$

Substituting equation (5) into equation (10) yields

$$\hat{w}(0,\hat{t})=\hat{w}(1,\hat{t})=0,\quad \left.\frac{\partial\hat{w}}{\partial\hat{x}}\right|_{(0,\hat{t})}=\left.\frac{\partial\hat{w}}{\partial\hat{x}}\right|_{(1,\hat{t})}=0 \tag{11}$$

3. Harmonic Vibration in Conduction Equation

Assuming a harmonic vibration in the nth mode shape in the form

$$\hat{w}(\hat{x},\hat{t})=\sum R_n(\hat{x})e^{i\Omega_n\hat{t}}\quad,\quad \hat{\theta}(\hat{x},\hat{z},\hat{t})=\sum\Theta_n(\hat{x},\hat{z})e^{i\Omega_n\hat{t}} \tag{12}$$

Where Ω_n is the frequency and $R_n(\hat{x})$ and $\Theta_n(\hat{x},\hat{z})$ are the nth mode shapes of the beam and the associated temperature variation respectively. Equations (12) are substituted into (7) and (9).

$$\frac{\partial^2\Theta_n(\hat{x},\hat{z})}{\partial\hat{z}^2}=i\Omega_n\alpha_5\Theta_n(\hat{x},\hat{z})-i\Omega_n\hat{z}\frac{\partial^2R_n(\hat{x})}{\partial\hat{x}^2} \tag{13}$$

$$\widehat{M}_n^T = \int_{-\frac{1}{2}}^{\frac{1}{2}} \hat{z}\Theta_n(\hat{x},\hat{z})d\hat{z}\ , \quad \widehat{N}_n^T = \int_{-\frac{1}{2}}^{\frac{1}{2}} \Theta_n(\hat{x},\hat{z})d\hat{z} \tag{14}$$

To solve equation (13), some boundary conditions are needed. These boundary conditions are $\partial\Theta_n/\partial\hat{z} = 0$ at $\hat{z} = \pm 1/2$ because the upper and lower surfaces of the beam are adiabatic and there is no flow heat across those surfaces. Then, solving equation (13), yields

$$\Theta_n(\hat{x},\hat{z}) = \frac{1}{\alpha_5}\frac{\partial^2 R_n(\hat{x})}{\partial\hat{x}^2}\left(\hat{z} - \frac{\sin(N_n\hat{z})}{N_n cos(N_n/2)}\right) \tag{15}$$

Where

$$N_n = (1-i)\sqrt{\frac{\Omega_n\alpha_5}{2}} \tag{16}$$

Substituting (15) into (14), yields

$$\widehat{M}_n^T = C_n^T\frac{\partial^2 R_n(\hat{x})}{\partial\hat{x}^2} \tag{17}$$

$$\widehat{N}_n^T = \frac{1}{\alpha_5}\frac{\partial^2 R_n(\hat{x})}{\partial\hat{x}^2}\left[\frac{\hat{z}^2}{2} + \frac{\cos(N_n\hat{z})}{N_n^2 cos(N_n/2)}\right]_{-\frac{1}{2}}^{\frac{1}{2}} = 0 \tag{18}$$

Where

$$C_n^T = \frac{1}{12\alpha_5}[1 + f(\Omega_n)] \tag{19}$$

$$f(\Omega_n) = \frac{24}{N_n^3}\left(\frac{N_n}{2} - tan\left(\frac{N_n}{2}\right)\right) \tag{20}$$

4. Nonlinear thermoelastic damping

In this section, the nonlinear thermoelastic damping is obtained by using the DQ method [36]. For this purpose, equation (6) is discretized based on the DQ method [36].

$$\frac{\partial^2}{\partial\hat{t}^2}\widehat{w}_i + \sum_{j=1}^{N} A_{ij}^{(4)}\widehat{w}_j + \alpha_1\left(\frac{\partial^2\widehat{M}^T}{\partial\hat{x}^2}\right)_i = \left(\sum_{j=1}^{N} A_{ij}^{(2)}\widehat{w}_j\right)\left\{\hat{P}_i - \sum_{i=1}^{N}\left[\alpha_6\left(\widehat{N}^T\right)_i - \alpha_2\left(\frac{\partial^2\widehat{M}^T}{\partial\hat{x}^2}\right)_i\sum_{j=1}^{N} A_{ij}^{(1)}\widehat{w}_j - \alpha_3\left(\sum_{j=1}^{N} A_{ij}^{(1)}\widehat{w}_j\right)^2\right]\right\} + \alpha_4\frac{{V_p}^2}{(1-\widehat{w}_i)^2} \tag{21}$$

Where

$$A_{ij}^{(1)} = \begin{cases} \dfrac{M(x_i)}{(x_i - x_j)M(x_j)} & i \neq j \\ -\displaystyle\sum_{j=1}^{N} A_{ij}^{(1)} & i = j \end{cases} \qquad i,j = 1,2,\dots,N \tag{22}$$

$$M(x_i) = \prod_{j=1\ j\neq 1}^{N}(x_i - x_j) \tag{23}$$

$$A_{ij}^{(r)} = \begin{cases} r\left[A_{ij}^{(r-1)}A_{ij}^{(1)} - \dfrac{A_{ij}^{(r-1)}}{x_i - x_j}\right] & i \neq j \\ -\displaystyle\sum_{j=1}^{N} A_{ij}^{(r)} & i = j \end{cases} \tag{24}$$

The last term in the right side of equation (21) representing the electric load, is expanded by Maclaurin series to M terms. Now, by applying harmonic vibration, relations (12), in the linear terms of (21) and substituting relations (17) and (18) into (21) the following equation is obtained.

$$-\Omega_n^2 R_i + \sum_{j=1}^{N} A_{ij}^{(4)} R_j + \alpha_1 C_n^T \sum_{j=1}^{N} A_{ij}^{(4)} R_j = \left(\sum_{j=1}^{N} A_{ij}^{(2)} R_j\right)\left\{\hat{P}_i + \sum_{i=1}^{N}\left[\alpha_2\left(\sum_{j=1}^{N} A_{ij}^{(4)} R_j\right)\sum_{j=1}^{N} A_{ij}^{(1)}\hat{w}_j + \alpha_3\left(\sum_{j=1}^{N} A_{ij}^{(1)}\hat{w}_j\right)^2\right]\right\} + \alpha_4 {V_p}^2\left(\sum_{m=2}^{M} m\,\hat{w}_i^{m-2}\right) R_i \quad (25)$$

The discretized clamped-clamped boundary condition is obtained as the following

$$R_1 = R_N = 0 \qquad \sum_{j=1}^{N} A_{1j}^{(1)} R_j = \sum_{j=1}^{N} A_{Nj}^{(1)} R_j = 0 \quad (26)$$

In order to solve the equations (25) and (26), a direct iterative method, which was presented in [36], is used. The real and imaginary parts of obtained nonlinear complex frequency are separated for calculating the thermoelastic damping

$$Q_n^{-1} = 2\left|\frac{Im(\Omega_n)}{Re(\Omega_n)}\right| \quad (27)$$

It is noted that by neglecting the nonlinear terms in equation (25) the linear model is achieved.

$$-\Omega_n^2 R_i + \sum_{j=1}^{N} A_{ij}^{(4)} R_j + \alpha_1 C_n^T \sum_{j=1}^{N} A_{ij}^{(4)} R_j = \left(\sum_{j=1}^{N} A_{ij}^{(2)} R_j\right)\hat{P}_i + 2\alpha_4 {V_p}^2 R_i \quad (28)$$

For calculating the static deflection due to electrical load the discretized and dynamic, equation (21) should be reduced to static form.

$$\sum_{j=1}^{N} A_{ij}^{(4)}\hat{w}_j = \left(\sum_{j=1}^{N} A_{ij}^{(2)}\hat{w}_j\right)\left\{\hat{P}_i + \sum_{i=1}^{N}\left[\alpha_3\left(\sum_{j=1}^{N} A_{ij}^{(1)}\hat{w}_j\right)^2\right]\right\} + \alpha_4\frac{{V_p}^2}{(1-\hat{w}_i)^2} \quad (29)$$

5. Validation of DQ Method

The validations of thermoelastic damping and stretching effects are done. For stretching effect validation, the electric load and thermoelastic damping are neglected and $\left({}^{\omega}/_{\omega_0}\right)^2$ is calculated and listed in Table 1 and compared with the results that are represented in Reference [38] where ω is the real part of nonlinear frequency, ω_0 is the real part of linear frequency, R is the mode shape in the middle of microbeam and r is the radius of gyration of the cross-section area.

Table 1.comparison between DQ method and [38]

R/r	FEM [38]	DQ method (N=24)	$\left\|\frac{FEM\ value - DQ\ value}{FEM\ value}\right\| \times 100$
0.6	1.0216	1.0204	0.1175
0.8	1.0383	1.0362	0.2023
1	1.0598	1.0566	0.3019
1.5	1.1343	1.1269	0.6524
2	1.2382	1.2246	1.0984
2.5	1.3708	1.3490	1.5903
3	1.5320	1.4996	2.1149

For thermoelastic damping validation, a microbeam whose properties are listed in Table 2, is considered. The calculated thermoelastic damping, as a function of beam thickness, h, illustrated in Fig. 2 and compared with Lifshitz and Roukes model [6]. This figure shows that the linear thermoelastic damping is obtained properly.

Table 2.properties of silicon microbeam

$T_0\ (K)$	$E\ (GPa)$	$\rho\ (kg\ m^{-3})$	ν	$\kappa\ (Wm^{-1}K^{-1})$	$d(\mu m)$	$L(\mu m)$
293	165.9	2330	0.22	156	2	700
$\alpha_T(10^{-6}K^{-1})$	$\hat{P}$	$c_v(Jkg^{-1}K^{-1})$	$\varepsilon(C^2m^{-2}N^{-1})$	$h(\mu m)$	$b(\mu m)$	$\Delta_E = E\alpha_T^2 T_0/c_v$
2.59	0	713	8.85×10^{-12}	5	5	0.4573

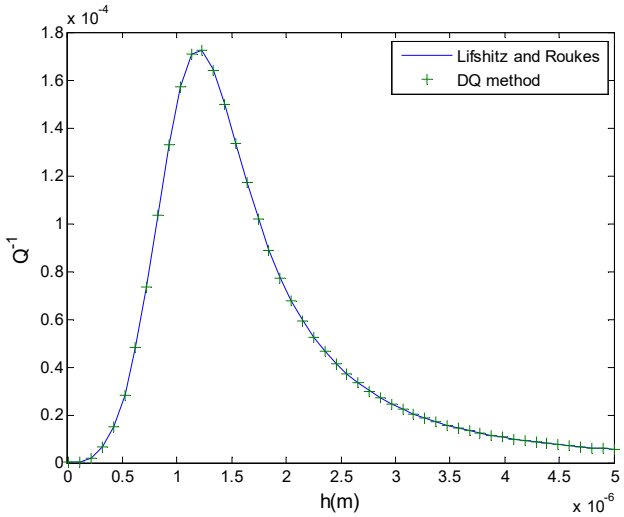

Fig. 2.comparison between Lifshitz and Roukes model [6] and DQ method

6. Results

All the results that are represented here are based on the data which listed in Table 2. In these results linear and nonlinear TED are compared with physical and geometrical parameters.

As approximated electrical load, the maximum value of m in equation (25) should be determined. Fig. 3 shows the variations of nonlinear TED versus m for both boundary conditions. As shown in this figure, beyond $m = 13$ the TED becomes constant so this value is chosen for approximation of the electrical load.

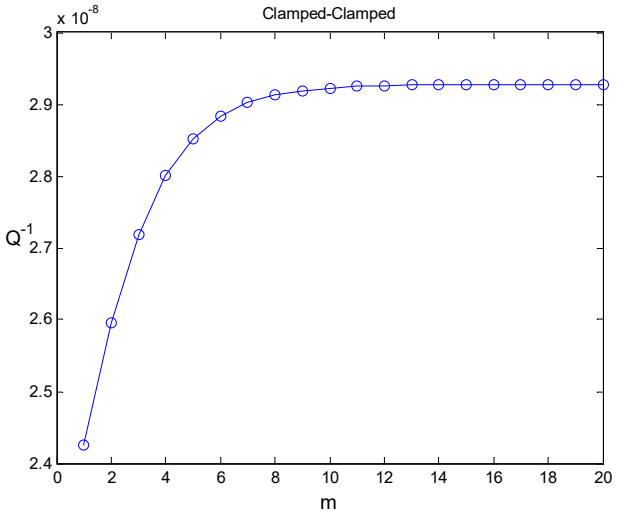

Fig. 3.variations of nonlinear TED versus m for clamped-clamped boundary conditions

Fig. 4 shows the variations of linear and nonlinear TED versus voltage. As can be seen in this figure, there is an obvious difference between linear and nonlinear models. For high value of voltage, the linear model cannot give the correct value of TED because the voltage increases the stretching effect of the microbeam (The first term in equation (25) represented this effect). Therefore, in the following results, for illustrating the differences between linear and nonlinear models, the comparisons between them are done at high values of voltages. There is also a difference in low values of voltages due to $\sum_{m=2}^{M} m\,\hat{w}_i^{m-2}$ that is multiplied by $\alpha_4 {V_p}^2$ in equation (25). The approximation of electrical load in equation (25) is more accurate than equation (28). Therefore, in low values of voltages, the nonlinear model is also more accurate. Also, for ensuring that the microbeam is not instable due to pull-in, the deflection of the microbeam center is depicted in this range of voltage in the Fig.5. The maximum deflection of the microbeam is 0.4 [16] for nonlinear model of the microbeam. As shown in Fig. 5 the deflection of the microbeam does not reach to maximum deflection, so pull-in instability does not occur.

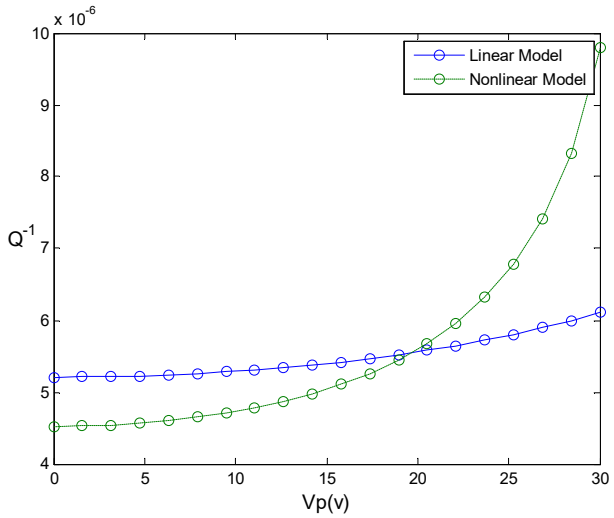

Fig. 4. Variations of linear and nonlinear TED versus voltage for $h = 5\mu m$

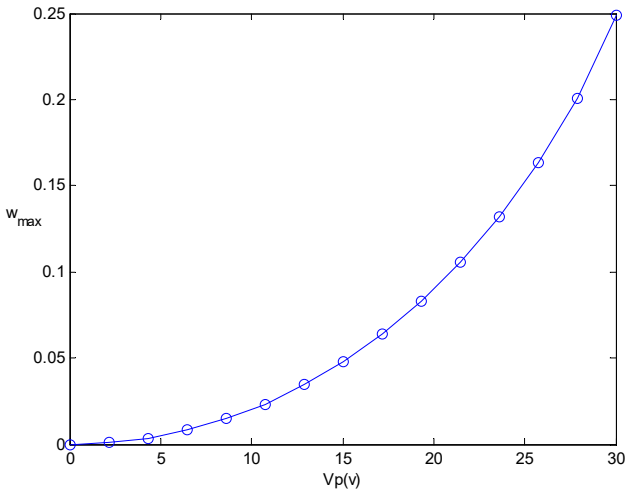

Fig. 5. Deflection of the center of the microbeam versus voltage

Fig.6 shows the TED versus thickness at $V_p = 30v$. In this case, there is small difference between the linear and nonlinear models. In both models, the critical thickness presented by [6] and [11] is observed. In the critical thickness TED has maximum value. If we want to investigate the effect of thickness, we should use the models in which the thick thickness is considered.

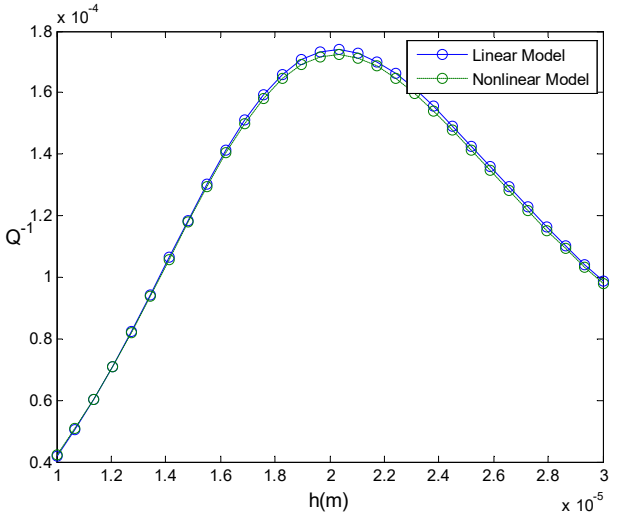

Fig.6. Variations of linear and nonlinear TED versus thickness for $V_p = 30v$

The variations of TED versus length is showed in Fig.7 by considering $V_p = 30v, h = 5\mu m$, according to this figure, the values of TED in nonlinear model are less than linear model especially in the maximum of TED. This different behavior is result of the integration of the second term through the length on the right side of equation (1). Therefore, the length can affect the stretching effect in the nonlinear model so the behavior of TED versus length is different in the linear and nonlinear models.

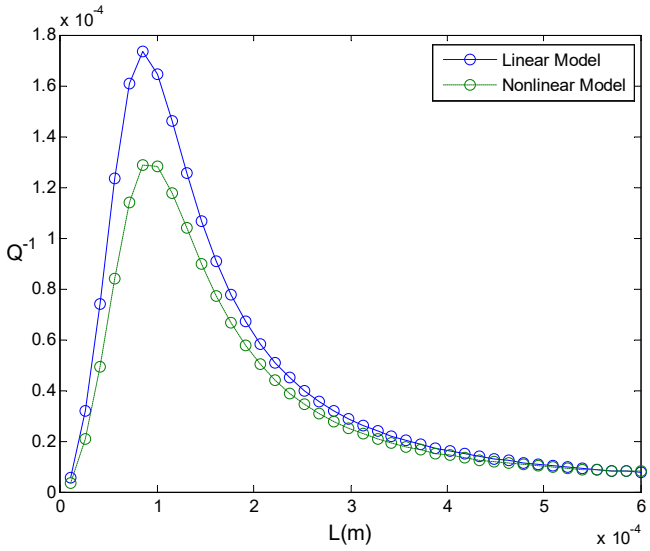

Fig.7.variations of linear and nonlinear TED versus length for $V_p = 30v, h = 5\mu m$

Fig.8 shows the variations of TED versus gap distance, d, by considering $V_p = 30v, h = 5\mu m\, L = 50\mu m$. According to this figure, behavior and values of TED in linear and nonlinear models are different. The TED in linear and nonlinear models starts at different values, as shown and discussed in Fig. 4, and for nonlinear one decreases. In the linear model, TED has constant behavior in this range of the gap distance. The gap distance affects the stretching effect due to electrical load so the nonlinear model has different value and behavior with respect to linear model.

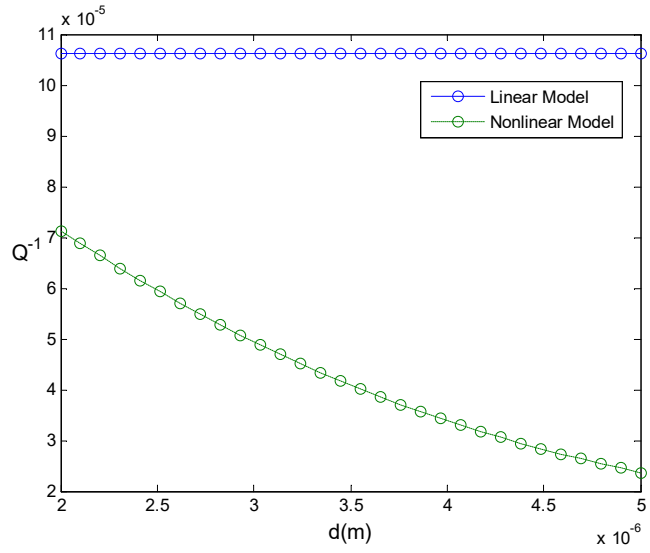

Fig.8.variations of linear and nonlinear TED versus gap distance for $V_p = 30v, h = 5\mu m$

Fig.9 shows the variation of TED versus $\hat{P}$. In both linear and nonlinear models by considering $V_p = 30v, h = 5\mu m$. As can be seen in this figure $\hat{P}$ has a little effect on the TED.

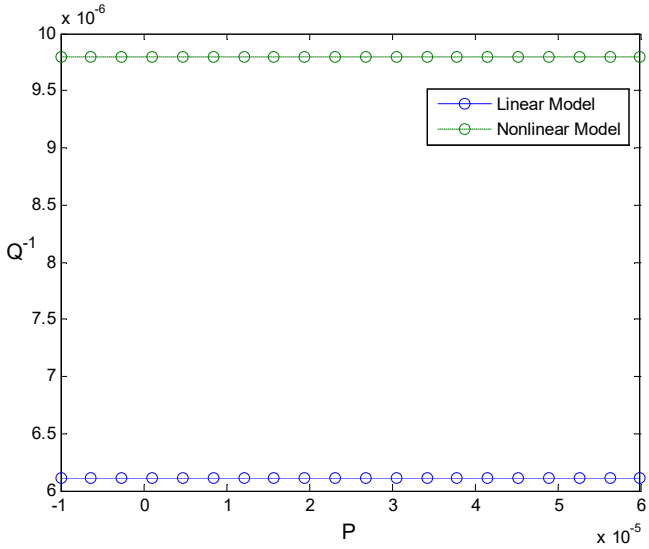

Fig.9.variations of linear and nonlinear TED versus $\hat{P}$ for $V_p = 30v, h = 5\mu m$

7. Conclusion

In this paper, it is shown that an applied voltage is a main nonlinear effect in MEMS resonators and at high values of voltage, as differences between linear and nonlinear model of MEMS resonators increase. Also, based on the obtained results, the TED variation versus length and gap distance, as the geometric parameters, have different behaviors in the linear and nonlinear models at high values of voltage because the voltage can intensify the stretching effect that is considered in nonlinear model. Therefore, at high values of voltage, the linear model cannot calculate the correct TED. In this case, the nonlinear model in which stretching effect is considered should be used.

References

[1] Ali H. Nayfeh, Mohammad I. Younis,"Modeling and simulations of thermoelastic damping in microplates", Journal of Micromechanics and Microengineering, 14 pp 1711–1717, 2004.
[2] Nayfeh A H and Younis M I.,"A new approach to the modeling and simulation of flexible microstructures under the effect of squeeze-film damping", Journal of Micromechanics and Microengineering, 14, pp 170–181, 2004.
[3] C. Zener,"Internal friction in solids I. Theory of internal friction in reeds", Physical Review, Volume 32, pp 230-235, 1937.
[4] C. Zener,"Internal friction in solids II. General theory of thermoelastic internal friction", Physical Review, Volume 53, pp 90-99, 1937.
[5] J. B. Alblas,"A note on the theory of thermoelastic damping", Journal of Thermal Stresses, Volume 4, Issue 3-4, pp 333-355, 1981.
[6] R. Lifshitz, M. L. Roukes, "Thermoelastic damping in micro- and nanomechanical systems", Physical Review B, Volume 61, Number 8, pp 5600-5609, 2000.
[7] Sudipto K. De, N. R. Aluru,"Theory of thermoelastic damping in electrostatically actuated microstructures", Physical Review B, 74, 144305, pp 1-13, 2006.
[8] S. Prabhakar, S. Vengallatore,"Theory of thermoelastic damping in micromechanical resonators with two-dimensional heat conduction", Journal of Microelectromechanical Systems, Vol. 17, No. 2, pp 494-502, 2008.
[9] Enrico Serra, and Michele Bonaldi,"A finite element formulation for thermoelastic damping analysis", International Journal for Numerical Methods in Engineering, 78, pp 671–691, 2009.
[10] F.L. Guo, G.A. Rogerson, "Thermoelastic coupling effect on a micro-machined beam resonator", Mechanics Research Communications, 30, pp 513–518, 2003.
[11] Yuxin Sun and Masumi Saka,"Thermoelastic damping in micro-scale circular plate resonators", Journal of Sound and Vibration 329, pp 328–337, 2009.
[12] Jinbok Choi, Maenghyo Cho, JaewookRhim,"Efficient prediction of the quality factors of micromechanical resonators", Journal of Sound and Vibration, 329, pp 84–95, 2010.
[13] Yun-Bo Yi, Mohammad A. Matin,"Eigenvalue Solution of Thermoelastic Damping in Beam Resonators Using a Finite Element Analysis", Journal of Vibration and Acoustics, Vol. 129, pp 478-483, 2007.
[14] FargasMarqu`es A, Costa Castell´o R and Shkel A M,"Modelling the electrostatic actuation of MEMS: state of the art" Technical Report, pp 1-33, 2005.
[15] R. C. Batra, M. Porfiri, and D. Spinello,"Review of modeling electrostatically actuated microelectromechanical systems", Smart Materials and Structures, 16, pp 23–31, 2007.

[16] Abdel-Rahman E. M., Younis M. I. and Nayfeh A. H.,"Characterization of the mechanical behavior of an electrically actuated microbeam", Journal of Micromechanics and Microengineering, 12, pp 759–66, 2002.
[17] Nayfeh A. H. and Younis M. I.,"Dynamics of MEMS resonators under superharmonic and subharmonic excitations", Journal of Micromechanics and Microengineering, 15, pp 1840–7, 2005.
[18]Younis M. I. and Nayfeh A. H., "A study of the nonlinear response of a resonant microbeam to an electric actuation", Nonlinear Dynamics, 31, pp 91–117, 2003.
[19] Younis M. I., Abdel-Rahman E. M. and Nayfeh A. H.,"A reduced-order model for electrically actuated microbeam-based MEMS", Journal ofMicroelectromech. System, 12, pp 672–80, 2003.
[20] Abdel-Rahman E. M. and Nayfeh A. H. "Secondary resonances of electrically actuated resonant microsensors", Journal of Micromechanics andMicroengineering. 13, pp 491–501, 2003.
[21] Nayfeh A. H. and Younis M. I.,"Dynamics of MEMS resonators under superharmonic and subharmonic excitations", Journal of Micromechanics and Microengineering, 15, pp 1840–7, 2005.
[22] Najar F., Choura S., Abdel-Rahman E. M., El-Borgi S. and Nayfeh A. H.,"Dynamic analysis of variable-geometry electrostatic microactuators", Journal of Micromechanics and Microengineering, 14, pp 900–6, 2006.
[23] Zhao X., Abdel-Rahman E. M. and Nayfeh A. H.,"A reduced-order model for electrically actuated microplates", Journal of Micromechanics and Microengineering, 14, pp 900–906, 2004.
[24] Vogl G. W. and Nayfeh A. H.,"A reduced-order model for electrically actuated clamped circular plates", Journal of Micromechanics and Microengineering, 15, pp 684–90, 2005.
[25] R.E. Bellman, J. Casti, "Differential quadrature and long term integration", Journal of Mathematical Analysis and Applications, Volume 34, 235–238, 1971.
[26] Feng Y., Bert CW., “Application of the quadrature method to flexural vibration analysis of a geometrically nonlinear beam”, Nonlinear Dynamics, Volume 156, pp 3-18, 1993.
[27] Guo Q. Zhong H., “Nonlinear vibration analysis of beams by a spline-based differential quadrature method”, Journal of Shock and Vibration, Volume 269, pp 413-420, 2004.
[28] Zhong H., Guo Q., “Nonlinear vibration analysis of Timoshenko beams using the differential quadrature method ”, Nonlinear Dynamics, Volume 32, pp 223-234.
[29] Han K. M., Xiao J. B., Du Z. M., “Differential quadrature method for Mindlin plates on Winkler foundations”, International Journal of Mechanical Sciences, Volume 38, pp 405-421, 1996.
[30] Liew K. M., Han J. B., Xiao Z. M., “Differential quadrature method for thick symmetric cross-ply laminates with first-order shear flexibility”, International Journal of Solids and Structures, Volume 33, pp 2647-2658, 1996.
[31] Liew K. M., Han J. B., “A four-node differential quadrature method for straight-sided quadrilateral Reissner/Mindlin plates”, Communications in Numerical Methods in Engineering, Volume 13, pp 73-81, 1997.
[32] Han J. B., Liew K. M., “An eight-node curvilinear differential quadrature formulation for Reissner/Mindlin plates”, Computer Methods in Applied Mechanics and Engineering, Volume 141, pp 265-280, 1997.
[33] P. Malekzadeh, “Differential quadrature large amplitude free vibration analysis of laminated skew plates based on FSDT”, Composite Structures, Volume 83, Issue 2, pp189-200, 2008.
[34] P. Malekzadeh, G. Karami, “Large amplitude flexural vibration analysis of tapered plates with edges elastically restrained against rotation using DQM”, Engineering Structures, Volume 30, Issue 10, pp 2850-2858, October 2008.
[35] P. Malekzadeh, “Three-dimensional free vibration analysis of thick functionally graded plates on elastic foundations”, Composite Structures, Volume 89, Issue 3, pp 367-373, July 2009.
[36] P. Malekzadeh, A.R. Vosoughi, “DQM large amplitude vibration of composite beams on nonlinear elastic foundations with restrained edges”, Communications in Nonlinear Science and Numerical Simulation, Volume 14, pp. 906–915, 2009.
[37] Nayfeh A. H., Frank P. P., linear and nonlinear structural mechanics, New Jersey, John Wiley & Sons, pp 215-225, 2004.
[38] B. S. Sarma and T. K. Varadan, “Lagrange-Type Formulation for Finite Element Analysis of Non-Linear Beam Vibrations”, Journal of sound and vibration, Volume 86, pp. 61-70, 1983.
[39] A. Koochi, Hamid M. Sedighi, M. Abadyan, "Modeling the size dependent pull-in instability of beam-type NEMS using strain gradient theory" Latin American Journal of Solids and Structures, Volume 11, pp. 1806-1829, 2014.
[40] A. Koochi, H. Hosseini-Toudeshky, H. R. Ovesy, "modeling the influence of surface effect on instability of nano-cantilever in presence of van der waals force" Volume 13, No. 4, 1250072, 2013.